# High-Performance Circular $TE_{01}$-Mode Converter

Ching-Fang Yu and Tsun-Hsu Chang, *Member, IEEE*

*Abstract*—This study presents the design and cold testing of a $Ka$-band $TE_{01}$-mode converter. A wave is efficiently converted from the $TE_{10}$ rectangular waveguide mode into the $TE_{01}$ circular waveguide mode. This converter comprises a power-dividing section and a mode-converting section. The field pattern and the working principle of each section are analyzed and discussed. A prototype was built and tested. Back-to-back transmission measurements exhibit excellent agreement to the results of computer simulations. The measured optimum transmissions are 97% with a 1-dB bandwidth of 5.8 GHz centered at 34.0 GHz. The angle-independent transmissions manifest high mode purity and the field pattern is directly demonstrated on a temperature-sensitive liquid-crystal sheet. In addition to exhibiting a high conversion efficiency, high mode purity, and broad bandwidth, this converter is also easy to construct and is structurally simple.

*Index Terms*—Converter, coupler, gyrotron, mode purity, wave launcher.

## I. INTRODUCTION

**T**HE $TE_{01}$ circular waveguide mode, featuring azimuthally symmetric electric field and low wall loss, has drawn much attention in relation to a variety of applications. These include electron-cyclotron maser-based devices, gyrotrons [1]–[13], plasma processing systems [14]–[16], and the next linear colliders and antennas [17], [18]. Gyrotrons require high-performance converters for many years. It launches a wave into an interaction circuit or couples the wave out for further applications. The performance of the mode converter directly affects the stability and tunability of the gyrotrons.

Means of generating a circular $TE_{01}$ mode can be classified into two categories according to the coupling methods involved. One is inline coupling [8], [11], [12], [14]–[23] and the other is sidewall coupling [2]–[5], [6], [7], [9], [10], [13], [24]. The former, using a deformed waveguide structure, gradually converts a wave into the desired mode. The transition length is typically long and multiple modes can be excited during the converting process. Among them, the Tantawi converter [6], [17], [19], Marie transducer [21], [22], serpentine/corrugated converter [8], [11], [20], and sector converter [23] are typical. In addition, Guo's converter [12], taking advantage of the wave nature, efficiently converts the waves between circular $TE_{01}$ and circular $TE_{02}$ modes. On the other hand, the latter generally uses a smooth waveguide with coupling holes on the
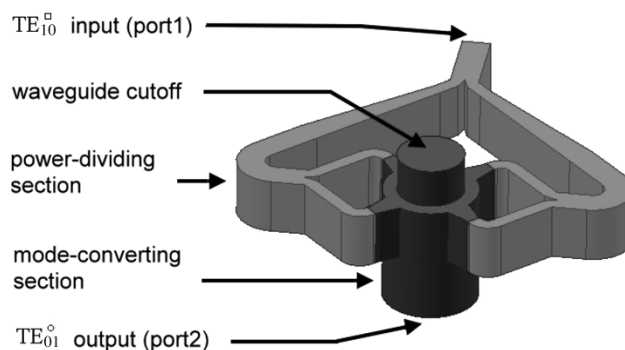


Fig. 1.  Schematic diagram of the $TE_{01}$-mode converter. The converter consists of two sections—the power-dividing section and mode-converting section.

sidewall. The typical coupling method is the multihole directional coupler, which is based on the field vector superposition theorem [3], [7]. Recently, coaxial couplers have been generally adopted because of their high converting efficiency [2], [4], [5], [10], [13], [24]. However, the existence of the unwanted modes during the transition could interact with an electron beam, resulting in a serious mode-competition problem for gyrotron applications. Thus, shortening the converting length and enhancing the mode purity help to eliminate the complicated mode-competition problem.

This study presents a sidewall coupling mode converter, which takes advantage of the wave nature to excite a pure $TE_{01}$ mode. This converter allows the electron beam to pass through it and to interact with the wave and, thus, it is especially suitable for gyrotron amplifier/oscillator applications. The rest of this paper is organized as follows. Section II shows the principle of operation and numerical results, and discusses the field forming processes and mode purity analysis. Section III describes fabrication and experimental results. Back-to-back measurements are present and field profiles are displayed. Finally, Section IV presents conclusions.

## II. PRINCIPLES AND SIMULATION

Fig. 1 schematically depicts the circular $TE_{01}$-mode converter, which is a two-port device. A wave injected into port 1 (rectangular waveguide $TE_{10}$ mode) is split into four signals of equal amplitude with special orientations in the power-dividing section. These four signals are then led into a circular waveguide in the mode-converting section to form a circular $TE_{01}$ mode, which will then emerge from port 2. Numerical simulation is conducted using a full-wave solver—High Frequency Structure Simulator (HFSS).[1]

[1]HFSS, Ansoft Corporation, Pittsburgh, PA. [Online]. Available: http://www.ansoft.com/
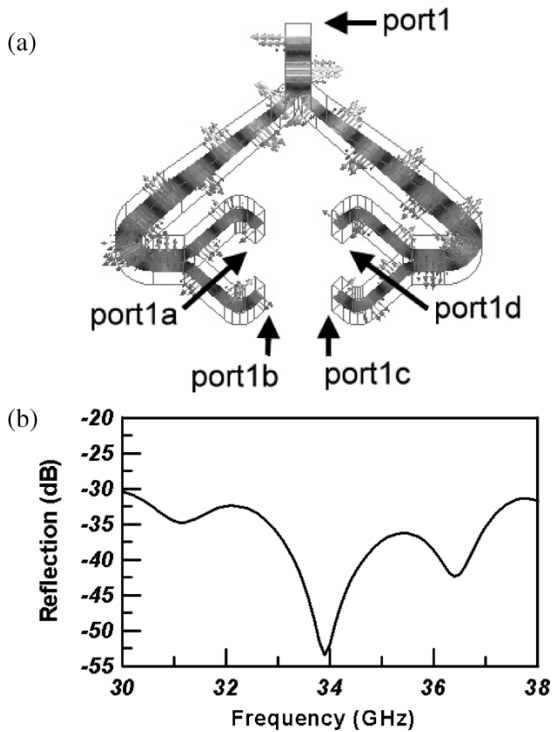
Fig. 2. HFSS simulation results. (a) Distribution of the electric-field strength of the power-dividing section viewed at the middle cross section of the rectangular waveguide. (b) Frequency response of the reflection at port 1; ports 1a–d are assumed to be matched to eliminate the effect of multiple reflections.



Fig. 3. (a) Cross-sectional view of the electric-field distribution with HFSS. (b) The reflection of port 2 with ports 2a–d matched.

### A. Power-Dividing Section

The input power is first divided into two signals of equal amplitude through a Y-shaped power divider. Each signal is then further divided through another Y-shaped power divider. Therefore, the cascaded Y-shaped power dividers quarter the input power. Fig. 2(a) shows the cross section of the electric-field distribution and the electric-field direction. The field strength is expressed as a grayscale image and the length of arrows. At the ends of the four output ports (ports 1a–d), the field strength are the same, but the electric-field orientations vary by 90°, indicating that all of the field strengths are the same, but the directions are counterclockwise, as viewed from the top. Such a power division is also discussed in [25] and [26].

Fig. 2(b) shows the reflection coefficient of the input port. Ports 1a–d are well terminated to prevent the complications caused by multiple reflections. Only the reflection at port 1 is examined. Optimizing the geometry of the Y-shaped splitters minimizes the reflection. The calculated reflection coefficient is better than 30 dB over the entire frequency range. Since the reflection of the power-dividing section is exceptional small, the mode-converting section determines the bandwidth of the coupler, as will be shown in Section II-B.

### B. Mode-Converting Section

Fig. 3(a) presents the outline of the mode-converting section and the cross section of the electric-field distribution. The field strength and direction are expressed in grayscale and by the directions of the arrows. The four signals of equal amplitude, but various orientations are injected into intermediary ports 2a–d.
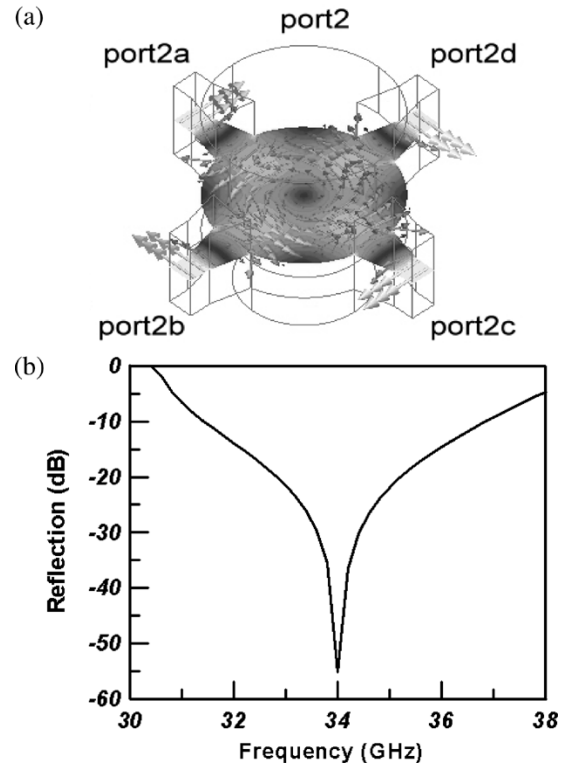
Sidewall coupling separates each by 90° along the circumference, forming the circular $TE_{01}$ waveguide mode. A microwave short (waveguide cutoff) is placed at the opposite end to ensure that the wave propagates in the desired direction. The resultant circular $TE_{01}$ wave emerges from port 2.

The microwave short is made of a circular waveguide of radius 4.2 mm with $TE_{01}$ cutoff frequency of 43.6 GHz. In gyrotron applications, this hole functions as the beam tunnel. Its diameter and position are optimized for the beam spot size and the wave transmission. In addition, a tapered geometry is used at the joints between the rectangular and circular waveguide, effectively minimizing the reflection. The principle concern in this section is to minimize the reflection at port 2, for which minimization can be achieved by optimizing the position of the waveguide cutoff and the joint geometry. Fig. 3(b) shows the optimized reflection in port 2, with ports 2a–d matched. The center frequency is 34 GHz and the −10-dB bandwidth is around 5.6 GHz.

### C. Analyzing Mode Purity

The next step is to put these two sections together. Fig. 4(a) shows the simulated electric-field strength of the converter on the surface and at the ports. This figure presents the mode-converting process. Given a radius of 6.0 mm, the cutoff frequencies for the first six modes are 14.7, 19.1, 24.3, 30.5, 30.5, and 33.4 GHz for $TE_{11}$, $TM_{01}$, $TE_{21}$, $TM_{11}$, $TE_{01}$, and $TE_{31}$, respectively. Therefore, when the desired $TE_{01}$ mode is being excited, the concentration of the other five modes shall be kept as low as possible. The sidewall couplings prevent the
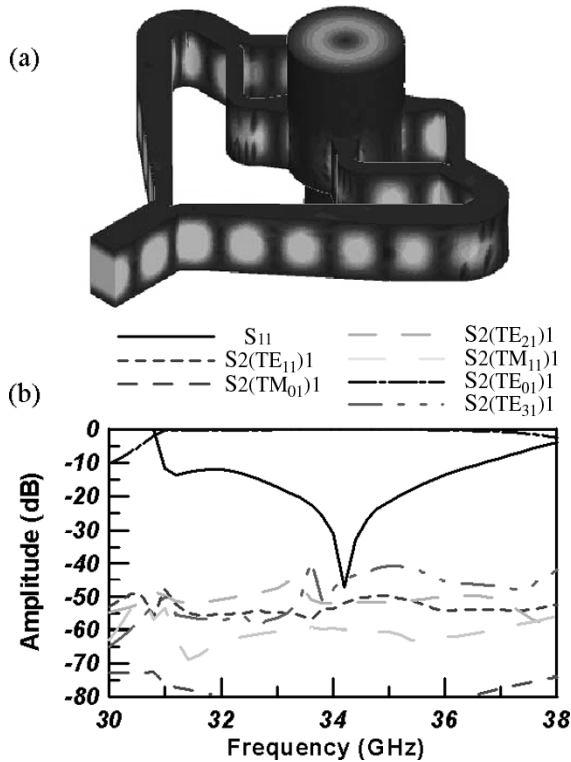
Fig. 4. (a) Electric-field strengths on the surface of the converter simulated with HFSS. (b) Calculated transmissions and reflection associated with a single converter.



Fig. 5. (a) Design drawings of the converter including a slotted plane (*left*) and plane cover (*right*). (b) The finished parts, which are made of OFHC copper.

excitations of TM waves because of the orientation of the electric field. Additionally, the quad-feed structure is unfavorable to the $TE_{11}$, $TE_{21}$, and $TE_{31}$ modes. It is instead suitable for a fourfold or a circular symmetric field pattern. In the range of operating frequencies, only the $TE_{01}$ mode can be formed. Therefore, high mode purity is expected.

Fig. 4(b) shows the transmission losses of the first six modes and the reflection loss at port 1. A $TE_{10}$ rectangular waveguide mode injected into port 1 was converted into six circular waveguide modes at port 2. The converting efficiency of a specific mode is defined as the output power of this mode at port 2 divided by the input power at port 1. The converting efficiency of the desired mode is very high and those of the other five modes are extremely low (below 0.01%). Close to the center frequency, the converting efficiency of the desired mode is approximately 98.5%. The remaining 1.5% is mainly because of reflection and ohmic loss. The concentrations of the spurious modes are basically less than −40 dB. Numerical calculations have shown an excellent performance. We are now in a position to verify these predictions.

## III. FABRICATION AND EXPERIMENTAL MEASUREMENT

Fig. 5(a) and (b) displays the design drawings and finished parts of the converter. The converter comprises two pieces—a slotted plate and a plane cover. It is made of oxygen-free high-conductivity (OFHC) copper. The slotted plate is machined using a computer numerically controlled (CNC) lathe with a tolerance of 0.01 mm. Plates are aligned with pins and
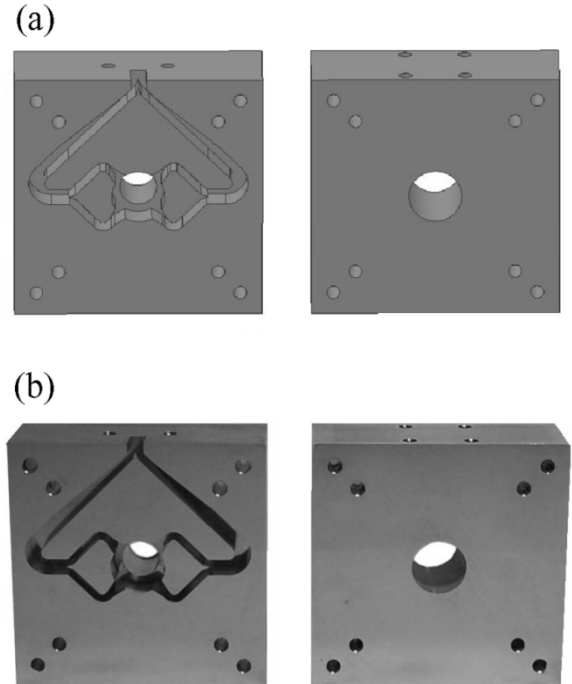
fastened with screws. In the cold test, two converters are joined back to back, which allows a direct measurement to be made using a two-port vector network analyzer (VNA), Agilent 8510C, Agilent Technologies, Palo Alto, CA.

### A. Back-to-Back Measurement

Fig. 6(a) shows the experimental setup. Two identical converters are joined back-to-back through a uniform middle section of 1.0 cm. A well-calibrated two-port VNA is employed. The measured results are highly consistent with the HFSS simulation data, as shown in Fig. 6(b). The bandwidths associated with the 1- and 3-dB transmission losses are 5.8 and 7.0 GHz, respectively. The measured converting efficiency of a single converter is approximately 98.5%. The ohmic loss and reflection account for the other is 1.5%. Measurements are made using a rotatable setup to further explore the field symmetry and to examine the existence of competing modes.

### B. Verifying Azimuthal Symmetry

Fig. 7(a) schematically depicts the experimental setup. The angle $\theta$ between the two identical converters can be adjusted. Three angles are used in this measurement. They are 0°, 45°, and 90°. Fig. 7(b) shows the measured results of transmission using these three setups. The transmission is almost independent of the angle for a broad bandwidth, which rules out the existence and circular polarization of the spurious modes. Thus, the excellent agreement between back-to-back measurements and the simulation was demonstrated. The next step is to display the field profile of the $TE_{01}$ mode in the circular waveguide associated with a single converter.
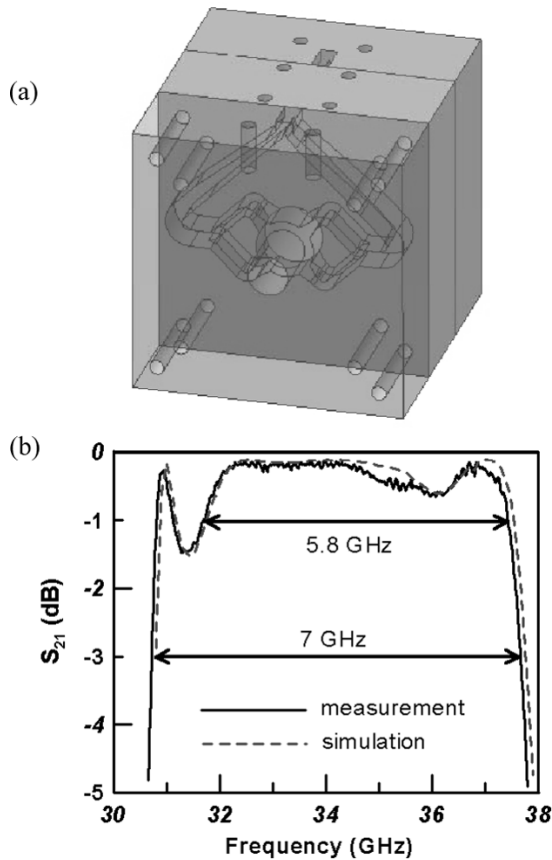
Fig. 6. (a) Two identical converters joined back to back. (b) Measured and simulated results of the back-to-back transmission.
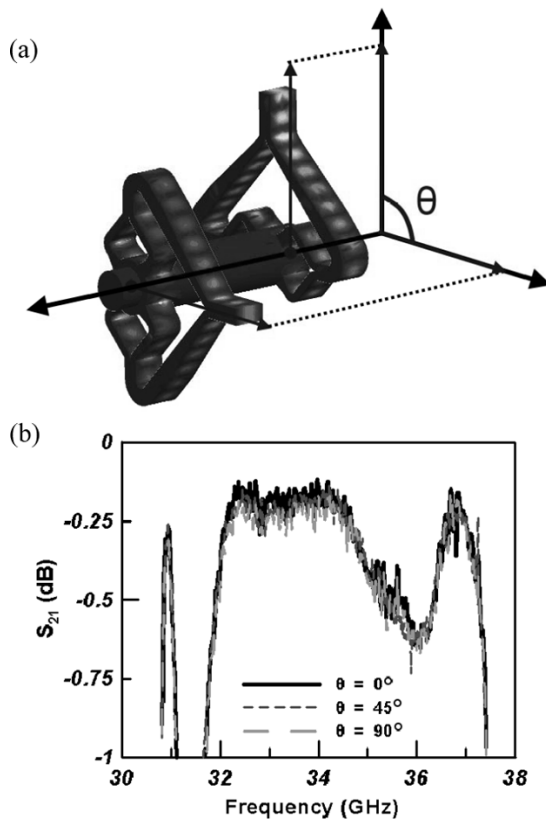


Fig. 7. (a) Drawing of the two converters jointed back to back and rotated at an angle of $\theta$. (b) The measured transmission results for three angles.
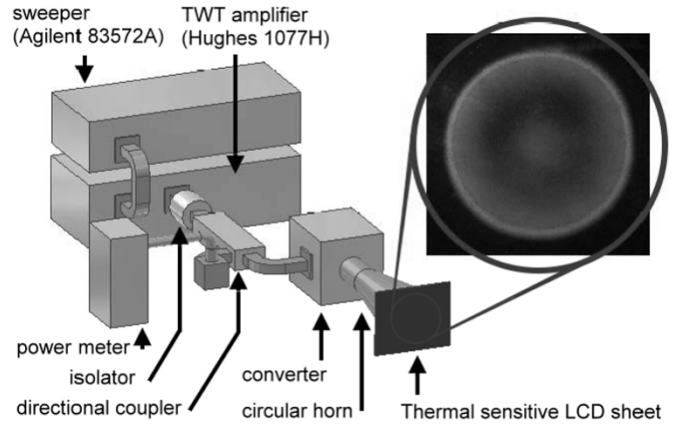


Fig. 8. Schematic diagram of the experimental setup for directly measuring the field distribution pattern. The power, generated by a TWT and controlled by a sweeper/synchronizer, is injected into the mode converter. A sheet of temperature-sensitive LCD is placed in front of the circular horn, where the grayscale image shows the time-averaged field distribution.

### C. Visualizing Field Profile

The following setup is used and measurements are made to visualize the field pattern directly. Fig. 8 schematically depicts the experimental setup and results. The microwave power is provided by the traveling-wave tube (TWT) amplifier (Hughes 1077H, Hughes, Germantown, MD) driven by a synchronizer (Agilent Technologies 8357a). An input power of 0.5 W, monitored using a calibrated circuit and power meter, is injected into the converter. A slightly tapered conical horn is connected at the end of the converter to enlarge the size of the field pattern for visual inspection. A temperature-sensitive liquid crystal display (LCD) sheet, displaying a full-color spectrum when the temperature changes from 25 °C to 30 °C, is placed in front of the horn. The color spectrum on the LCD is directly correlated with the microwave energy pattern. Fig. 8 displays the circular and azimuthal symmetric field pattern as evidence of the purity of the circular TE$_{01}$ mode.

### IV. CONCLUSION

A $Ka$-band circular TE$_{01}$-mode converter has been developed, fabricated, and tested. This converter features high back-to-back converting efficiency (97%), high mode purity (99.99%), compact converting section ($\sim 1.5\lambda_g$), and broad bandwidth (17% at a 1-dB transmission). Such a converter is suitable for a variety of applications, especially the gyrotrons. Although the presence of the electron beam might slightly change the performance of the converter, a $W$-band TE$_{01}$ gyrotron backward-wave oscillator (gyro-BWO) is being developed based on this converter.

### ACKNOWLEDGMENT

## REFERENCES

[1] K. R. Chu, "The electron cyclotron maser," *Rev. Mod. Phys.*, vol. 76, no. 2, pp. 489–540, Apr. 2004.

[2] M. Blank, B. G. Danly, and B. Levush, "Experimental demonstration of a $W$-band (94 GHz) gyrotwystron amplifier," *IEEE Trans. Plasma Sci.*, vol. 27, no. 2, pp. 405–411, Apr. 1999.

[3] K. C. Leou, D. B. McDermott, A. J. Balkcum, and N. C. Luhmann, Jr., "Stable high-power $TE_{01}$ gyro-TWT amplifiers," *IEEE Trans. Plasma Sci.*, vol. 22, no. 5, pp. 585–592, Oct. 1994.

[4] M. Garven, J. P. Calame, B. G. Danly, K. T. Nguyen, B. Levush, F. N. Wood, and D. E. Pershing, "A gyrotron-traveling wave tube amplifier experiment with a ceramic loaded interaction region," *IEEE Trans. Plasma Sci.*, vol. 30, no. 3, pp. 885–893, Jun. 2002.

[5] D. B. McDermott, H. H. Song, Y. Hirata, A. T. Lin, L. R. Barnett, T. H. Chang, H. L. Hsu, P. S. Marandos, J. S. Lee, K. R. Chu, and N. C. Luhmann, Jr., "Design of a $W$-band $TE_{01}$ mode gyrotron traveling-wave amplifier with high power and broad-band capabilities," *IEEE Trans. Plasma Sci.*, vol. 30, no. 3, pp. 894–902, Jun. 2002.

[6] J. P. Tate, H. Guo, M. Naiman, L. Chen, and V. L. Granatstein, "Experimental proof-of-principle results on a mode-selective input coupler for gyrotron applications," *IEEE Trans. Microw. Theory Tech.*, vol. 42, no. 8, pp. 1910–1917, Aug. 1994.

[7] W. Wang, Y. Gong, G. Yu, L. Yue, and J. Sun, "Mode discriminator based on mode-selective coupling," *IEEE Trans. Microw. Theory Tech.*, vol. 51, no. 1, pp. 55–63, Jan. 2003.

[8] W. Lawson, M. R. Arjona, B. P. Hogan, and R. L. Ives, "The design of serpentine-mode converters for high-power microwave applications," *IEEE Trans. Microw. Theory Tech.*, vol. 48, no. 5, pp. 809–814, May 2000.

[9] T. A. Spencer, C. E. Davis, K. J. Hendricks, F. J. Agee, and R. M. Gilgenbach, "Results from gyrotron backward wave oscillator experiments utilizing a high-current high-voltage annular electron beam," *IEEE Trans. Plasma Sci.*, vol. 24, no. 3, pp. 630–635, Jun. 1996.

[10] M. Blank, B. G. Danly, B. Levush, P. E. Latham, and D. E. Pershing, "Experimental demonstration of a $W$-band gyroklystron amplifier," *Phys. Rev. Lett.*, vol. 79, no. 22, pp. 4485–4488, Dec. 1997.

[11] M. J. Buckley and R. J. Vernon, "Compact quasi-periodic and aperiodic $TE_{0n}$ mode converters in overmoded circular waveguides for use with gyrotrons," *IEEE Trans. Microw. Theory Tech.*, vol. 38, no. 6, pp. 712–721, Jun. 1990.

[12] H. Guo, S. H. Chen, V. L. Granatstein, J. Rodgers, G. S. Nusinovich, M. T. Walter, J. Zhao, and W. Chen, "Operation of a high performance, harmonic-multiplying, inverted gyrotwystron," *IEEE Trans. Plasma Sci.*, vol. 26, no. 3, pp. 451–460, Jun. 1998.

[13] B. Levush, M. Blank, J. Calame, B. Danly, K. Nguyen, D. Pershing, S. Cooke, P. Latham, J. Petillo, and T. Antonsen, Jr., "Modeling and design of millimeter wave gyroklystrons," *Phys. Plasmas*, vol. 6, no. 5, pp. 2233–2240, May 1999.

[14] R. L. Kinder and M. J. Kushner, "$TE_{01}$ excitation of electron cyclotron resonance plasma source," *IEEE Trans. Plasma Sci.*, vol. 27, no. 1, pp. 64–65, Feb. 1999.

[15] Y. Kato, H. Furuki, T. Asaji, and S. Ishii, "Production of multicharged ions in a 2.45 GHz electron cyclotron resonance source directly excited in a circular $TE_{01}$ mode cavity resonator," *Rev. Sci. Instrum.*, vol. 75, no. 5, pp. 1470–1472, 2004.

[16] R. Hidaka, N. Hirotsu, N. Tanaka, and Y. Kawai, "Generation of electron cyclotron resonance plasmas using a circular $TE_{01}$ mode microwave," *J. Appl. Phys.*, vol. 72, no. 9, pp. 4461–4462, Nov. 1992.

[17] S. G. Tantawi, C. Nantista, N. Kroll, Z. Li, R. Miller, R. Ruth, and P. Wilson, "Multimoded RF delay line distribution system for the next linear collider," *Phy. Rev. ST Accel. Beams*, vol. 5, 032001, 2002.

[18] R. D. Wengenroth, "A mode transducing antenna," *IEEE Trans. Microw. Theory Tech.*, vol. MTT-26, no. 5, pp. 332–334, May 1978.

[19] I. Spassovsky, E. S. Gouveia, S. G. Tantawi, B. P. Hogan, W. Lawson, and V. L. Granatstein, "Design and cold testing of a compact $TE_{01}$ to $TE_{20}$ mode converter," *IEEE Trans. Plasma Sci.*, vol. 30, no. 3, pp. 787–793, Jun. 2002.

[20] M. J. Buckley, D. A. Stein, and R. J. Vernon, "A single-period $TE_{02}$-$TE_{01}$ mode converter in a highly overmoded circular waveguide," *IEEE Trans. Microw. Theory Tech.*, vol. 39, no. 8, pp. 1301–1306, Aug. 1991.

[21] G. R. P. Marie, "Mode transforming waveguide transition," U.S. Patent 2 859 412, Nov. 4, 1958.

[22] W. A. Huting and K. J. Webb, "Comparison of mode-matching and differential equation techniques in the analysis of waveguide transitions," *IEEE Trans. Microw. Theory Tech.*, vol. 39, no. 2, pp. 280–286, Feb. 1991.

[23] F. Sporleder and H. G. Unger, *Waveguide Tapers Transitions and Couplers*. New York: Peregrinus, 1979, ch. 7.

[24] A. H. McCurdy and J. J. Choi, *Design and Analysis of a Coaxial Coupler for a 35-GHz Gyroklystron Amplifier*, vol. 47, no. 2, pp. 164–175, Feb. 1999.

[25] R. J. Barker, N. C. Luhmann, Jr., J. H. Booske, and G. S. Nusinovich, *Modern Microwave and Millimeter-Wave Power Electronics*. Piscataway, NJ: IEEE Press, 2005, ch. 11.

[26] T. H. Chang and C. F. Yu, "Polarization controllable $TE_{21}$ mode converter," *Rev. Sci. Instrum.*, vol. 76, 074703, 2005.
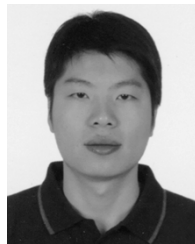
**Ching-Fang Yu** was born in Taipei, Taiwan, R.O.C., in 1978. He received the B.S. degree in physics from National Cheng Kung University, Taiwan, R.O.C., in 2000, the M.S. degree in physics from National Tsing Hua University, Taiwan, R.O.C., in 2002, and is currently working toward the Ph.D. degree in physics at National Tsing Hua University.

His current research includes the design, construction, and characterization of high-order-mode converters and their applications to gyro-BWOs.
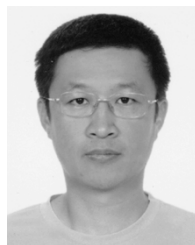
**Tsun-Hsu Chang** (M'99) received the B.S. degree from National Central University, Taoyuan, Taiwan, R.O.C., in 1991, and the Ph.D. degree from National Tsing Hua University, Hsinchu, Taiwan, R.O.C., in 1999.

Upon graduation, he was a Post-Doctoral Researcher involved with the development of high-power millimeter-wave sources (gyrotrons) for two years. From 2001 to 2003, he was a Technical Manager with the Silicon Integrated System Corporation, where he was responsible for analyzing high-speed signals and power integrity. He is currently an Assistant Professor with the Department of Physics, National Tsing Hua University. His current research focuses on the nonlinear dynamics and nonstationary behavior of the electron cyclotron maser and characterizes microwave/nanoparticles interaction.